21, rue d'Artois, F-75008 PARIS
http : //www.cigre.org

CIGRE US National Committee
2016 Grid of the Future Symposium

# Analysis of the Coupling Between Power System Topology and Operating Condition for Synthetic Test Case Validation

**E. SCHWEITZER*** Arizona State University USA

**A. SCAGLIONE** Arizona State University USA

**R. THOMAS** Cornell University USA

**T. OVERBYE** University of Illinois Urbana-Champaign USA

## SUMMARY

In this paper we observe a statistical trend coupling the driving point impedance seen at a power system node and the magnitude of power injection at that node. Based on this relation a criterion to validate synthetic transmission grid samples could be developed with the intent of ensuring that researchers using such synthetic cases as surrogates for the real cases can draw realistic conclusions in their studies. The basic operating hypothesis of our study is that sample grids and operating conditions are coupled and cannot be independently assigned. Our intuition, which is proven to be a real statistical trend, is that this is due to the well-known inversely proportional relationship between power and impedance. This statistical trend can be turned into a validation method, since emulating the impedance characteristics of real grids through synthetic samples and assigning operating conditions that also reflect this coupling is a method to offer guarantees of observing realistic trends in the analysis of ensemble properties of the states calculated via the synthetic grids.

## KEYWORDS

Driving Point Impedance, Power System Test Cases, Statistical Analysis

*Eran.Schweitzer@asu.edu
The information, data, or work presented herein was funded in part by the Advanced Research Projects Agency-Energy {ARPA-E), U.S. Department of Energy, under Award Number DE-AR0000714. The views and opinions of authors expressed herein do not necessarily state or reflect those of the United States Government or any agency thereof.

## INTRODUCTION

There is increasing recognition that synthetic models for power grids are needed [1] [2] [3], including at the institutional level through programs like Grid Data from ARPA-E[1]. A primary motivation for such models is the lack of access to data, either for reasons of security, or due to companies' proprietary data concerns. However, models are necessary for any type of power system simulation, and for testing and development of new grid applications. Therefore, creating realistic models would fulfill a real need in the community.

Test cases provide a sample feasible operating point along with the electrical characteristics. The operating points are the inputs to the system, the classic ones being real and reactive power for load buses and real power and voltage magnitude for generator buses. The corresponding outputs related to a positive sequence power flow are voltage magnitudes and angles for load buses, and voltage angle and reactive power injection for generator buses. A researcher using a synthetic case would expect to have operating points and electrical characteristics that, in concert, allow him/her to observe power flow results, i.e. outputs, that have similar trends as those of "real" test cases.

Our working hypothesis is that the electrical characteristics and feasible (as well as typical) operating conditions are coupled. To the best of our knowledge, the first work that pointed out and substantiated this claim is [4]. The prior art did not provide an explanation for this coupling.

Our goal in this paper is to provide a justifiable relationship between electrical characteristics and the placement and magnitude of both positive and negative injection in a sample grid. Our goal is to use this notion as part of a validation methodology for synthetic transmission grid models: in fact, if the electrical parameters in a synthetic case are statistically similar to real test cases and if the operating conditions are coupled to these parameters in a statistically similar way as in the real test cases, then the synthetic case should be considered as a realistic surrogate for the real case since it will produce similarly distributed state variables. Next we explain the basic intuition that lead us to identify how the sample electrical systems and operating points are coupled.

## I. BASIC INTUITION

Considering our working hypothesis, the goal is to find a sufficiently simple guiding principle relating feasible and typical operating conditions to the electrical parameters and topology of the system. Note that this principle is meant to suggest and justify a statistical trend, not to be an exact law.

Our basic intuition is as follows. Considering the relationship between power and Impedance:

$$P = \frac{|V|^2 \cos(\theta)}{|Z|} \Rightarrow P \propto |Z|^{-1} \tag{1}$$

$$Q = \frac{|V|^2 \sin(\theta)}{|Z|} \Rightarrow Q \propto |Z|^{-1} \tag{2}$$

where $\cos(\theta)$ is the power factor. We note that the diagonal entry of the $Z$ matrix, $Z_{i,i}$ is the Thévenin equivalent impedance seen by node $i$. A crude and oversimplified view of load or generation at any given node would be to consider an impedance, $Z_{inj} = |V_i|^2/S_i$, in series with the Thévenin impedance. The logical conclusion that follows from this, is that more power could be generated or consumed at lower total impedance, i.e. at nodes with lower, $Z_{i,i}$. Furthermore, we would expect the relationship to follow some sort of power law with a negative exponent around $-1$. We should emphasize that the scope of the analysis present focuses on meshed transmission system. While the

[1] http://arpa-e.energy.gov/?q=arpa-e-programs/grid-data

intuition holds for lower voltages and radial systems, these simplified structures allow more certainty and therefore will likely merit a modified approach.

## II. RESULTS & ANALYSIS

Before examining the relationship between power and impedance, we consider the distribution of driving-point impedances, $Z_{i,i}$, for different test cases in Figure 1. Overall, all the cases largely follow a similar trend, which suggest this is an intrinsic characteristic of transmission systems. It should be noted that the range of magnitudes is in part dependent on what is modeled in the system. For example, including the generator step up transformers increases the overall magnitude. However, we can expect a similar sort of distribution overall, simply shifted.

Building on the intuition from Section I, we also note that the ERCOT case[2] has several impedances that are larger by almost an order of magnitude than the rest of the cases. This would suggest that these nodes would be particularly poor points in the system for both power generation and consumption. Therefore, to continue insuring a viable system while providing a synthetic case to be used as a surrogate of the ERCOT case with an acceptable power flow solution, even more (negative) correlation between power and driving point impedance would be forced than in the other cases in Figure 1.

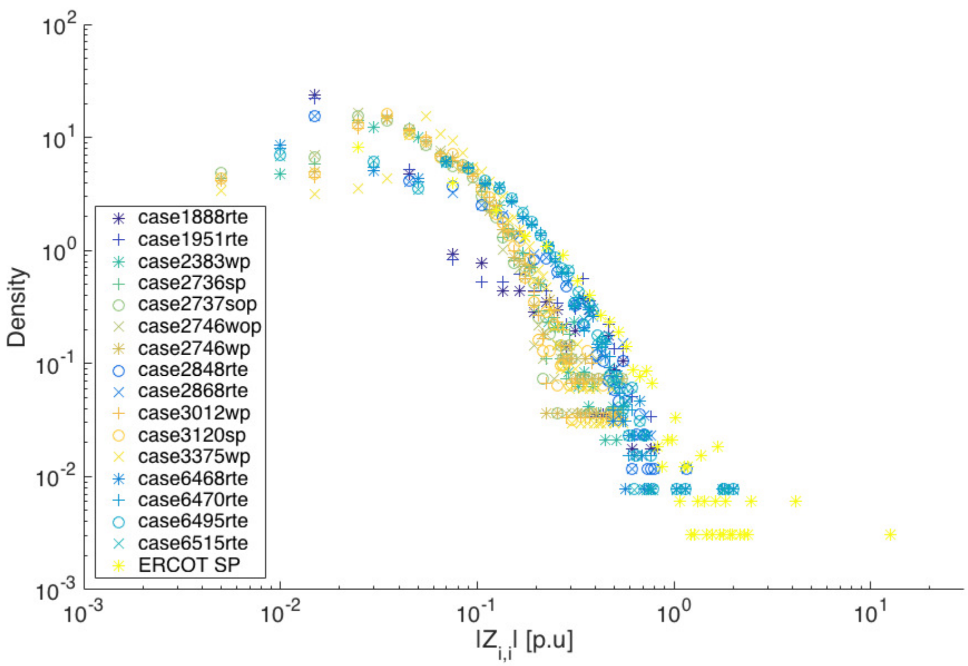


*Figure 1 Histogram of driving point impedance for various test cases*

Next, the correlation we conjectured above is tested by separating each power injection vector into 6 parts, namely:

1. $P_g$: Real Power Generation
2. $P_d$: Real Power Demand
3. $P_{net}$: Net Real Power ($P_g - P_d$)
4. $Q_g$: Reactive Power Generation
5. $Q_d$: Reactive Power Demand
6. $Q_{net}$: Net Reactive Power ($Q_g - Q_{net}$)

[2] ERCOT case data was obtained as part of a FERC freedom of information request

In all cases the *magnitude* is considered rather than the resulting signed value. This is because we wish to consider these relationships on a log scale, where the power law relationship we conjectured in Section I appears as a linear trend with negative slope. Additionally, the magnitudes of power possible to consume or produce at a given node is of interest and therefore, the sign is not critical. Finally, for each comparison, only nodes with non-zero power injection are considered.

The scatter plots in Figure 2 provide an overview of the analysis which follows. For space reasons only the ERCOT case and a 6515 bus RTE case available with Matpower [5] are presented. Their similarity is meant to underline that all the figures share certain characteristics. First of all, we note that there is clearly a non-negligible correlation between the different power vector parts and the driving point impedance.

This correlation is shown in Figure 3 for all of the cases. Of particular note are the levels of the correlation coefficients. For example, It is clear from both Figure 2 and Figure 3 that real power generation is more strongly negatively correlated with the driving point impedance than the other quantities. However, what Figure 3 demonstrates is that each of the six correlations considered is fairly contained within a range. Additionally, as hypothesized based on the impedance histogram, the correlation coefficient for power generation $P_g$ is a bit larger for the ERCOT case than for the others.

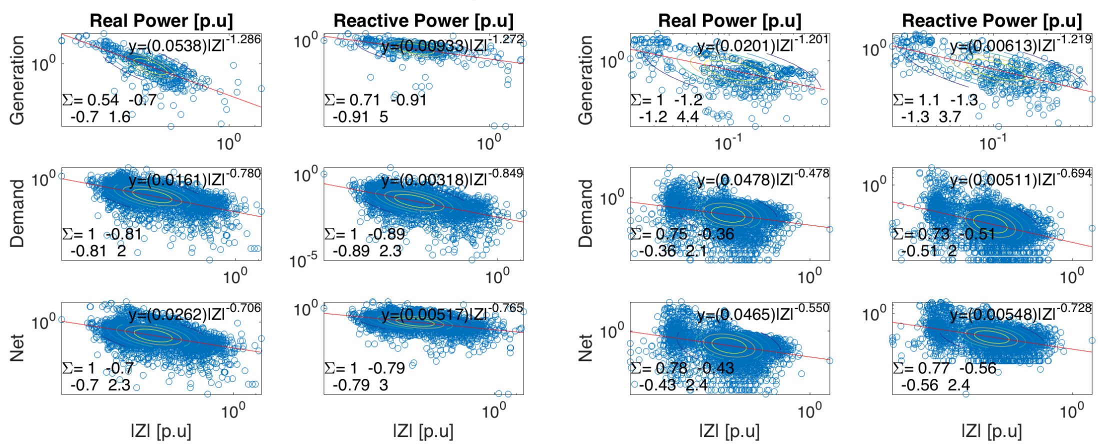


*Figure 2 Scatter plots of power injection vectors vs. driving point impedance in log-log scale for the ERCOT case (left) and RTE 6515 Matpower Case (right). Additionally, the power-law fit line, and bivariate normal distribution fit contour lines are shown*

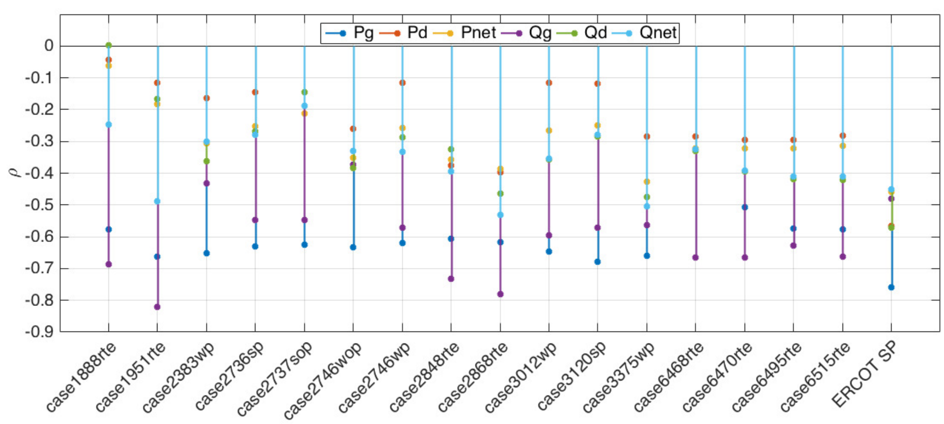


*Figure 3 Correlation coefficients between driving point impedance at a node and the power injections at that same node.*

Figure 2 also contains power law fit lines in red for each of the scatter plots. While it is clear that the points do not simply lie on a line, the fit does provide some insight into the overall trend. The equation for these lines in the linear space would be

$$|y| = e^{b}|Z|^{m}, \tag{3}$$

where $y$ stands for each of the 6 power vector components considered. These equations are printed on the figures and we note that particularly for generation nodes, $m \approx -1$, which fits with the intuition provided by (1) and (2).

The linear fit is clearly insufficient to describe the relationship between power and impedance. However, it also acts as the major axis of level planes for a bivariate normal distribution fit to the data. The bivariate normal is defined by two elements $\mu$ and $\Sigma$:

$$\mu = \begin{bmatrix} \mu_{\ln|Z|} & \mu_{\ln|y|} \end{bmatrix} \quad (4)$$

$$\Sigma = \begin{bmatrix} \sigma^2_{\ln|Z|} & -\rho\sigma_{\ln|Z|}\sigma_{\ln|Z|} \\ -\rho\sigma_{\ln|Z|}\sigma_{\ln|Z|} & \sigma^2_{\ln|y|} \end{bmatrix}, \quad (5)$$

where $y$ is again each of the 6 power vector components considered. It is a natural next step to consider the lack of conformity to the correlation as noisy variation from the trend. A simple way to proceed after such an interpretation is fitting a bivariate normal distribution, whose contour plots are also shown in Figure 2.

To better visualize and assess how well the bivariate normal fit matches the data Figure 4 overlays it on top of the bivariate histogram of the real power injections and the driving point impedance. Overall, the fit is quite reasonable, especially for $P_g$ (top left). The plots for the demand and net vectors suggest that perhaps fitting a bimodal distribution would be preferable, however, that is currently left for future work.

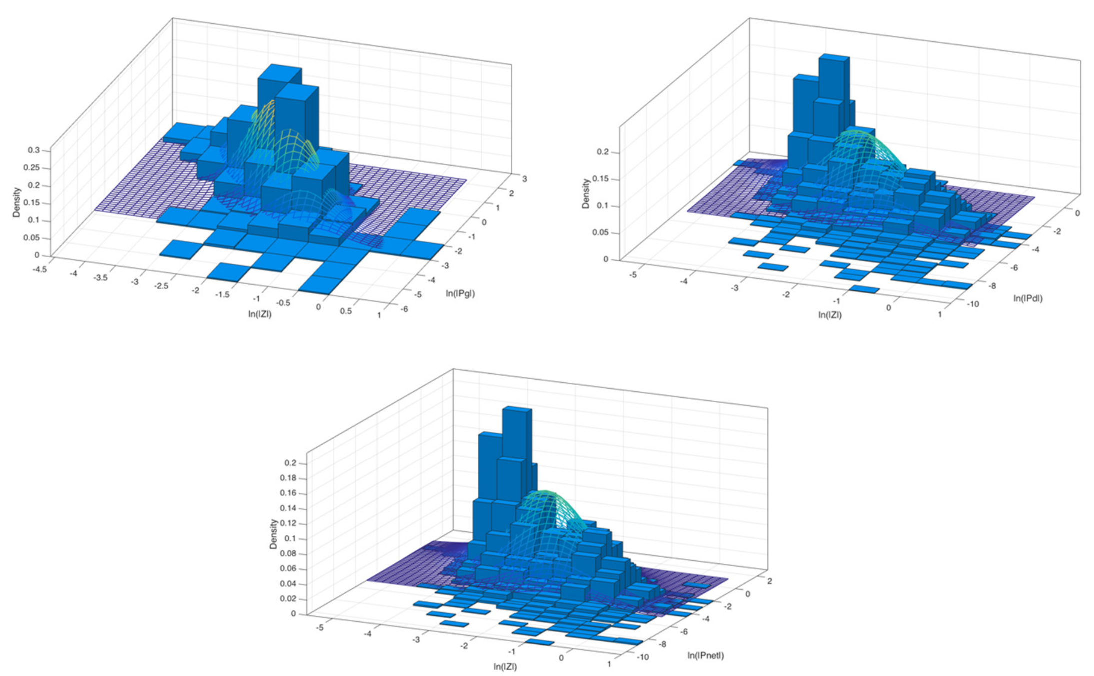


*Figure 4 ERCOT case bivariate normal distribution plotted over the bivariate histogram of driving point impedance and real power generation (top left), real power demand (top right), and net power injection (bottom). Plots for reactive power quantities are quite similar.*

As a final analysis, we consider how the possible fitting variables $(\rho, b, m, \Sigma, \mu)$ relate to one another and themselves for the cases considered. Figure 5 shows an array of plots where each of these variables are compared to each of the other ones. Along the diagonal, a histogram of the value is given. Again only the plot for $P_g$ is given for space reasons, however, the other plots are similar in spirit. A few observations are offered:

1. There does *not* appear to be any correlation with the system size, $N$. This is important since one can extrapolate that the same trend exists for very large systems.
2. Most of the histograms are fairly tightly centered around a mean.
3. The covariance term (last column of Figure 5) is fairly independent of all other variables besides the two variances.

The combination of observation 2 and 3 supports the conclusion that there is a probabilistic relationship between the driving point impedance at a system node and its power injection. The implications are discussed in the following section.

## III. DISCUSSION

The trends and relationships demonstrated in the previous section indicate the nature of coupling between topology and load in a power system. The driving point impedance, seen as the Thévenin equivalent, encapsulates electrical topological information within it. Furthermore, the impedance matrix can be obtained as the inverse of the admittance matrix[3], which is constructed from the primal branch admittances. Therefore, if the primal elements, i.e. individual branches of a system, are appropriately connected, the resulting driving point impedances will also be correct. The analysis presented here suggests that for every such correct topology, there is a simple method to allocate power injections, such that the resulting case will match reality. Specifically, the load and generation should roughly follow the bivariate normal distribution with respect to the driving point impedance. These results also help motivate recent publications that identified strong correlation between topological features and bus type assignment [4] [6] [7]. These papers found that, while repeated permutations result in a normal distribution of the so-called Bus Type Entropy, $w$, the value, $w^*$, associated with the real test case lies far on the tails of the distribution. Our analysis offers a physical intuition to this observation. Namely, power injections are correlated to the topology via the driving point impedance. A random assignment of power injections (which is the same as assigning bus type except that magnitude is also involved) ignores this correlation and is therefore unlikely to correctly reproduce it.

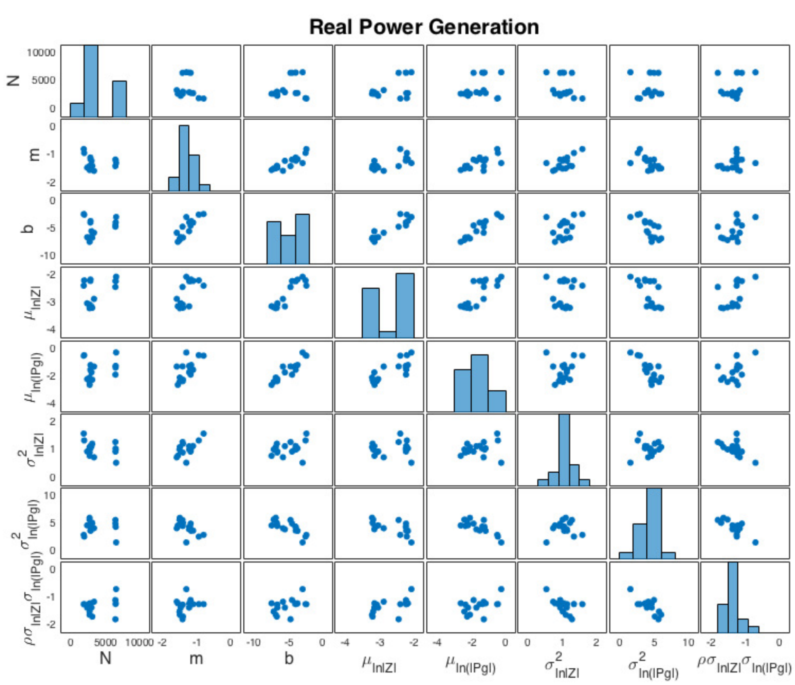


*Figure 5 Relationship between the various fitting variables used to analyze the correlation of power and driving point impedance. N is the system size.*

[3] This is not an efficient way to calculate the impedance matrix, however it is useful from an analysis perspective

Some observations along these lines were made in [8] regarding the so-called Electrical distance, which is simply $|Z|$. Our work refines these notions by focusing only on the diagonal, which is largely looked over in [8], as the most critical indicator of possible loading at a system node.

This investigation is motivated by a search for meaningful validation criteria for synthetic test cases where positive sequence power flow is concerned. The proposed metric is the correlation between the driving point impedances of the system and the power injections. The following variables would be considered

1. $\rho$: the correlation coefficient between power injections and driving point impedances.
2. $m$: the exponent in the best fit line to the power law function between the power injections and driving point impedances.
3. $\mu$: mean of the log of power injections and driving point impedances.
4. $\Sigma$: the covariance matrix of the log of power injections and driving point impedances.

If the test case is supposed to emulate a specific system, comparison to that specific system could suffice. If, on the other hand, a more general verification is desired, the result can be compared to histograms such as those in Figure 5. The more a synthetic case falls in the middle of these distributions, the more it displays a realistic and normal operational point with respect to its topology and its electrical grid parameters. These similarities can be quantified via various divergence tests that compare the distributions of synthetic and real grids. The numerical result would then be included in a weighted evaluation of the full list of validation tests.

## IV. CONCLUSION

This paper analyzes the relationship between driving point impedances in a system and the power injections for the system. An intuitive derivation presents the expected nature of the relationship, and subsequent analysis shows that results indeed match the trend at large. Finally, a rough outline is proposed for how synthetic test cases could benefit from these results both in validating the test cases as well as in guiding some elements of their generation. This direction will be pursued in future work.

**BIBLIOGRAPHY**


[1] Z. Wang, A. Scaglione, and R. Thomas, “Generating Statistically Correct Random Topologies for Testing Smart Grid Communication and Control Networks,” *IEEE Transactions on Smart Grid,* pp. 28-39, June 2010.

[2] KP Schneider *et. al*., “Modern Grid Initiative Distribution Taxonomy Final Report,” Richland, WA, 2008.

[3] K. Gegner, A. Birchfield, T. Xu, K. Shetye, and T. Overbye, “A Methodology for the Creation of Geographically Realistic Synthetic Power Flow Models” *Power and Energy Conference at Illinois (PECI)*, Urbana, IL, 2016.

[4] Z. Wang, S. Elyas, and R. Thomas, “A Novel Measure to Characterize Bus Type Assignments of Realistic Power Grids,” *IEEE PowerTech 2015* , Eindhoven, 2015.

[5] R.D. Zimmerman, C.E. Murillo-Sánchez, and R.J. Thomas, “MATPOWER: Steady-State Operations, Planning, and Analysis Tools for Power System Research and Education,” *IEEE Transactions on Power Systems,* vol. 26, no. 11, pp. 12-19, 2011.

[6] S. Elyas, and Z. Wang, “A Multi-Objective Optimization Algorithm for Bus Type Assignment in Random Topology Power Grid Model,” *49th HICSS*, 2015.

[7] Z. Wang, R. Thomas, “On Bus Type Assignment in Random Topology Power Grid Models,” *48th HICSS*, 2015.

[8] E. Cotilla Sanchez, P. Hinse, C. Barrows, and S. Blumsack “Comparing the Topological and Electrical Structure of the North American Electric Power Infrastructure,” *IEEE Systems Journal*, vol. 6, no. 4, pp. 616-626, 2012.